Supporting Information

for

Quantitative Predictions of Molecular Diffusion in Binary Mixed-Linker Zeolitic Imidazolate Frameworks Using Molecular Simulations

Ross J. Verploegh[1,‡], Ying Wu[1,2,‡], Salah Eddine Boulfelfel[1], David S. Sholl[1,*]

[1]*School of Chemical & Biomolecular Engineering, Georgia Institute of Technology, Atlanta, GA 30332-0100*

[2]*The School of Chemistry and Chemical Engineering, South China University of Technology, Guangzhou, Guangdong, People's Republic of China 510641*

***CORRESPONDING AUTHOR:** david.sholl@chbe.gatech.edu

Table of Contents

Adsorbate Force Fields and Adsorbate-Framework Interactions

We modeled SF_6 as a single-site 12-6 Lennard-Jones (LJ) fluid[1] and N_2 as a 3-site rigid linear molecule[2-3]. We modeled methanol, ethanol, 1-butanol, methane, propane, n-butane, and isobutane using the united atom TraPPE FF.[4-6] The single and double C-C bonds were modeled with a harmonic potential[7], a departure from the original TraPPE implementation to facilitate implementation in LAMMPS. The OPLS force field was used to model rigid benzene (C_6H_6).[8-9] We have also included H_2O modeled using the SPC/E FF designed to work with long range electrostatic solvers (Ewald)[10-11]. **Table S1** shows all the adsorbate LJ parameters and **Table S2** shows all the ZIF 12-6 Lennard-Jones parameters used only to describe framework-adsorbate interactions. For those seeking to replicate these calculations, the bond lengths, angles, and dihedrals used are in the original references.

Table S1. Adsorbate force field parameters along with molecular diameters (KD=kinetic diameter, vdW=van der Waals diameter, and LJ=diameter approximated from Lennard-Jones sigma parameters) and molecular weights.

Index	Adsorbate	Molecular Diameter [Å]	LJ Site (name)	MW [g mol^{-1}]	σ [Å]	ε [kcal mol^{-1}]	ε [K]	q [e]
1	SF_6	5.13[LJ]	SF_6	146.06	5.13	0.4414	222.1	0.0
2	N_2	3.64[KD,12]	2xN_{N2}	14.01	3.32	0.0724	36.43	-0.482
			N_{COM}	0.00	0.0	0.0	0.0	+0.964
3	H_2O	2.89[vdWD]	O_{H2O}	16.00	3.166	0.15535	78.18	-0.8476
			2xH_{H2O}	1.01	0.0	0.0	0.0	0.4238
4	CH_3OH	3.60[vdWD,13]	CH_3_sp3[a]	15.03	3.750	0.1947	98.0	0.265
			O	16.00	3.020	0.1848	93.0	-0.700
			H	1.01	0.0	0.0	0.0	0.435
5	C_2H_5OH	4.10[KD,14]	CH_3_sp3	15.03	3.750	0.1947	98.0	0.0
			CH_2_sp3[a]	14.02	3.950	0.0914	46.0	0.265
			O	16.00	3.020	0.1848	93.0	-0.700
			H	1.01	0.0	0.0	0.0	0.435
6	CH_4	3.25[vdWD,12]	CH_4	16.04	3.73	0.2941	148.0	0.0
7	C_3H_8	4.16[vdWD,12]	CH_3	15.03	3.750	0.1947	98.0	0.0
			CH_2	14.02	3.950	0.0914	46.0	0.0
8	n-C_4H_{10}	4.52[vdWD,12]	2x CH_3	15.03	3.750	0.1947	98.0	0.0
			2xCH_2	14.02	3.950	0.0914	46.0	0.0
9	iso-C_4H_{10}	5.0[KD,12]	CH_3_sp3	15.03	3.750	0.1947	98.0	0.0
			CH_sp3	13.02	4.680	0.0199	10.0	0.0

Table S.1 continued								
10	C_6H_6	5.80[KD,13]	6xC_xyl	12.01	3.55	0.0700	35.24	-0.115
			6xH_xyl	1.01	2.42	0.0299	15.03	0.115
11	1-butanol	4.5[LJ]	CH_3	15.03	3.75	0.1947	98.0	0.00
			$2xCH_2$	14.02	3.95	0.0914	46.0	0.00
			CH_2_sp3[a]	14.02	3.95	0.0914	46.0	0.265
			O	16.00	3.02	0.1848	93.0	-0.700
			H	1.01	0.0	0.0	0.0	0.435

Table S2. 12-6 Lennard-Jones parameters on framework atoms used to model adsorbate-framework interactions.

Atom Type	ε [kcal/mol]	σ [Å]
Zn	0.067	2.462
N	0.037	3.261
C_x	0.057	3.431
H_x	0.024	2.571
O	0.032	3.118

Potential Energy Comparisons between PBE-D3(BJ) and the AMBER and intraZIF Force Fields

Table S3 shows the statistics used to benchmark the AMBER and intraZIF force fields at predicting configurational potential energies from fully periodic Born-Oppenheimer Molecular Dynamics (BOMD) simulations. The mean absolute error (MAE), mean signed deviation (MSD), root mean squared deviation (RMSD), and the normalized root mean squared deviation (NRMSD) are reported. The NRMSD is defined as the RMSD divided by the standard deviation of the PBE-D3(BJ) energies and is reported as a percentage.

Table S3. Statistics benchmarking the quality of the AMBER and intraZIF force fields at describing PBE-D3(BJ) configurational potential energies from BOMD simulations at 700 K and 1.01 bar. Units are in kJ mol^{-1} Zn^{-1}. The statistics for the AMBER force field are in the parentheses.

Material	MAE	MSD	RMSD	NRMSD	N samples
ZIF-8	8.99 (55.51)	-8.17 (+55.51)	10.72 (56.87)	45.32 (240.41)	5550
ZIF-8_{75}-90_{25}	7.33 (67.44)	+0.09 (+67.44)	9.03 (83.84)	45.96 (426.78)	4708
ZIF-8_{50}-90_{50}	9.02 (59.58)	+6.64 (+59.58)	11.54 (68.95)	72.94 (435.91)	5250
ZIF-8_{25}-90_{75}	16.62 (46.13)	+16.46 (+46.13)	18.89 (50.69)	166.85 (447.65)*	5509
ZIF-90	15.38 (50.87)	+15.25 (+50.87)	17.24 (52.47)	81.20 (247.03)	6099

**The NRMSD for ZIF-8_{25}-90_{75} is larger than ZIF-90 because a lower standard deviation of the PBE-D3(BJ) energies was observed.*

Mean Squared Displacement Analysis from NPT-MD Simulations of Methane in ZIF-8-90

Figure S1 below shows MSD plots for methane measured over the composition range of ZIF-8-90 materials. Methane diffusion in ZIF-90 is faster than in ZIF-8.

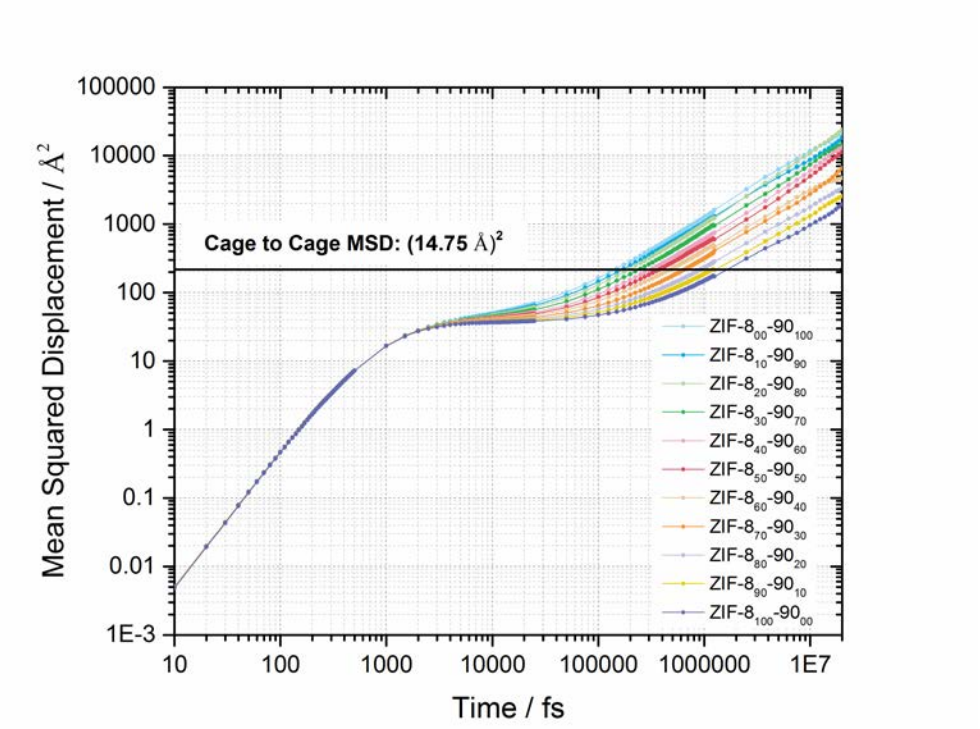

Figure S1. MSDs for CH_4 in ZIF-8-90 where the square of the cage to cage distance is indicated by the solid black line. These MSDs were calculated at a loading of two methane molecules per unit cell (one molecule per cage), 308 K, and 1.01 bar.

Hopping Rates of N-Butane, 1-Butanol, and Isobutane in ZIF-8-90

Figure S2 below shows the hopping rates of n-butane, 1-butanol, and isobutane in the four window types of ZIF-8-90. A type 1 window contains 3 mIm linkers and a type 4 window contains 3 ImCA linkers as described in the main manuscript.

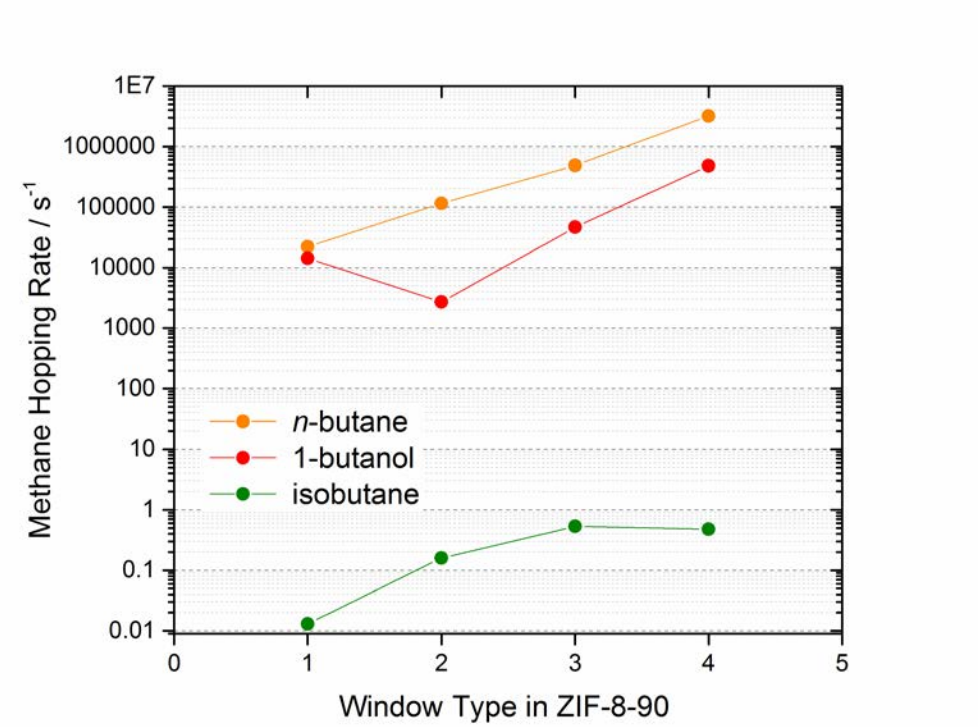

Figure S2. Hopping rates of n-butane, 1-butanol, and isobutane through ZIF-8-90 window types at 308 K and 1.01 bar.

Ideal Diffusion Selectivities in SALEM-2/ZIF-8 Hybrids

Figure S3 below shows the n-butane/isobutane ideal diffusion selectivities experimentally measured[15] and simulated for SALEM-2/ZIF-8 hybrids. **Figure S4** shows the ideal diffusion selectivities for combinations of benzene, isobutane, and SF_6 in SALEM-2/ZIF-8 hybrids at 308 K and 1.01 bar.

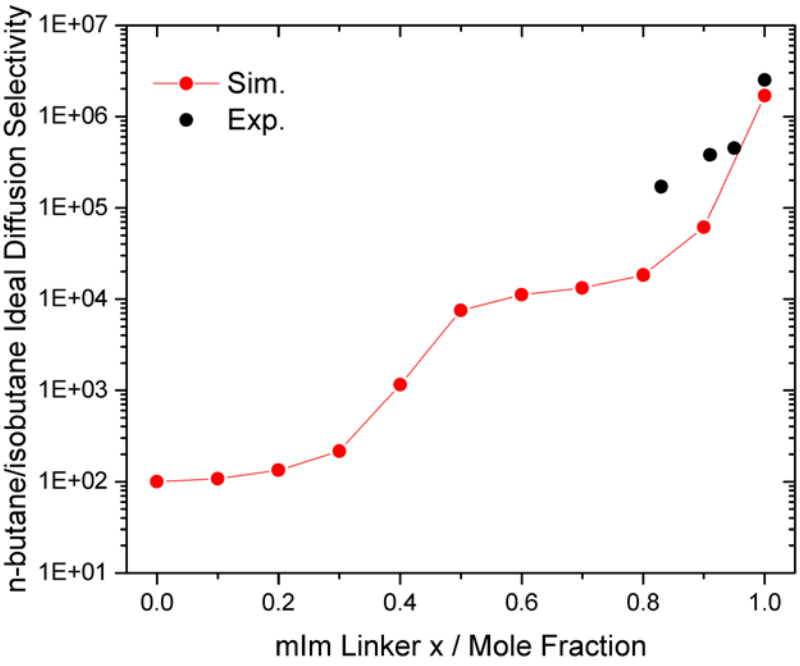

Figure S3. Ideal n-butane/isobutane diffusion selectivity as a function of mIm linker in SALEM-2/ZIF-8 hybrids with a SRO α=0 (red circles) at 308 K and 1.01 bar. The ideal diffusion selectivities measured by Zhang and Koros at the same conditions are shown as solid black circles.[15] Lines are guides for the eye.

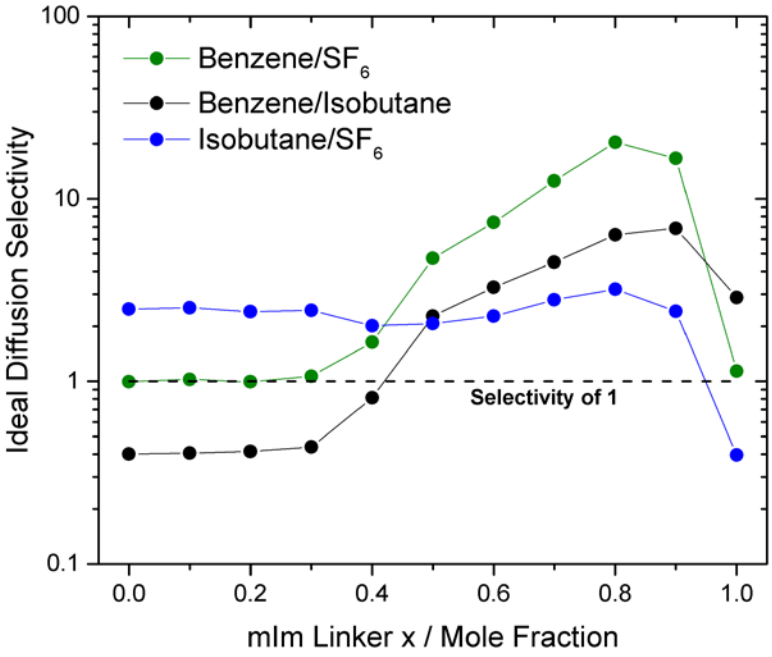

Figure S4. Predicted ideal diffusion selectivities of combinations of benzene, isobutane, and SF_6 in SALEM-2/ZIF-8 hybrids at 308 K and 1.01 bar. The dashed line indicates a selectivity of 1. Lines are guides for the eye.

Grand Canonical Monte Carlo Simulations for SALEM-2/ZIF-8 Hybrids

Grand Canonical Monte Carlo (GCMC) was performed using the RASPA-2.0[16] simulation code to simulate n-butane, isobutane, and SF_6 adsorption isotherms in SALEM-2/ZIF-8 hybrids. **Figure S5** reports the isotherms along with corresponding thermodynamic correction factors for SALEM-2/ZIF-8 with varying composition and random SRO (α=0). The SALEM-2/ZIF-8 hybrids were modeled as rigid structures, which were first energy minimized in LAMMPS using the intraZIF-FF. The Peng-Robinson equation of state was used to covert fugacities to pressures with critical pressures, critical temperatures, and acentric factors for n-butane and isobutane taken from the RASPA-2.0 source code (originally from the NIST database). The critical pressure and critical temperature for SF_6 was taken from the NSIT database, but the acentric factor of SF_6 was taken from the website of Isidoro Martinez (http://webserver.dmt.upm.es/~isidoro/). A total of 150,000 MC cycles were used for initialization and 150,000 MC cycles were used for the production period. Pretabulated energy grids were generated with a 0.15 Å spacing to enhance computational efficiency. **Table S4** reports the thermodynamic correction factors evaluated at a bulk pressure of 0.03 bar for n-butane, isobutane, and SF_6 across the entire SALEM-2/ZIF-8 composition range. **Tables S5-S7** reported the experimental transport diffusivities, the simulated thermodynamic correction factors (TCF), and the calculated corrected diffusivities for n-butane, isobutane, and SF_6. The thermodynamic correction factors were linearly interpolated from the ZIF-8 and ZIF-Im_{25}-mIm_{75} isotherms.

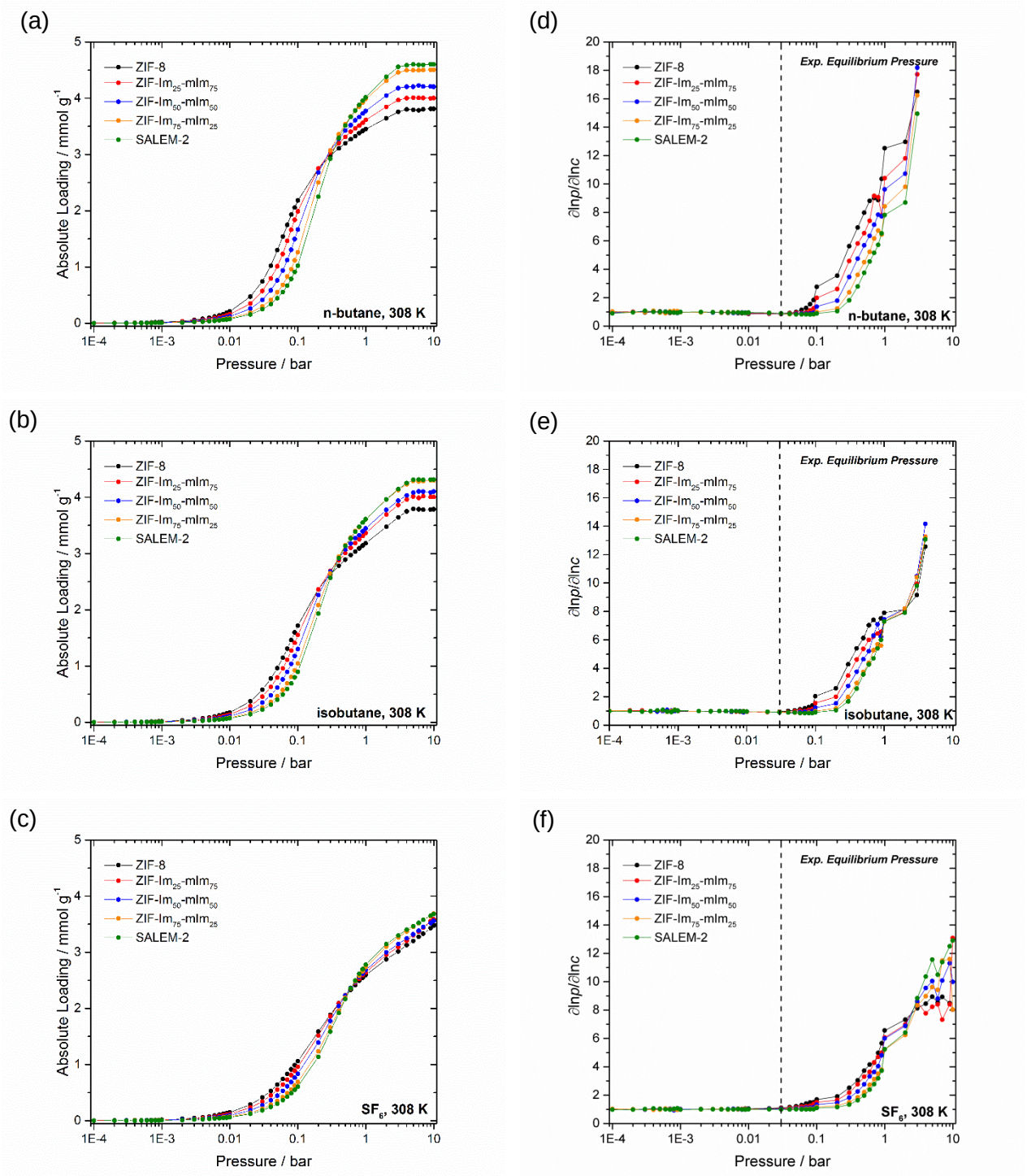

Figure S5. **(a-c)** Simulated adsorption isotherms of n-butane, isobutane, and SF_6 and **(d-f)** corresponding thermodynamic correction factors at 308 K. The dashed line in plots d-f represents the assumed experimental equilibration pressure of 0.03 bar as inferred from pressure decay measurements by Eum et al.[17]

Table S4. Thermodynamic correction factors for n-butane, isobutane, and SF_6 in ZIF-8/SALEM-2 hybrid materials at a bulk pressure of 0.03 bar and 308 K.

ZIF	n-butane	isobutane	SF_6
ZIF-8	0.90	0.94	1.11
ZIF-Im_{25}-mIm_{75}	0.84	0.90	1.06
ZIF-Im_{50}-mIm_{50}	0.85	0.89	1.03
ZIF-Im_{75}-mIm_{25}	0.87	0.90	0.99
SALEM-2	0.89	0.90	0.99

Table S5. Corrected diffusivities of n-butane in ZIF-8/SALEM-2 hybrids calculated from the experimental transport diffusivities reported by Zhang and Koros[15] and the thermodynamic correction factors taken from simulated adsorption isotherms at 308 K.

ZIF	D_T [$cm^2\ s^{-1}$]	TCF [-]	D_0 [$cm^2\ s^{-1}$]
ZIF-8	5.7×10^{-12}	0.90	5.1×10^{-12}
ZIF-Im_{02}-mIm_{98}	Not reported	-	-
ZIF-Im_{05}-mIm_{95}	7.7×10^{-12}	0.89	6.9×10^{-12}
ZIF-Im_{09}-mIm_{91}	1.1×10^{-11}	0.88	1.0×10^{-11}
ZIF-Im_{17}-mIm_{83}	1.6×10^{-10}	0.86	1.4×10^{-10}

Table S6. Corrected diffusivities of isobutane in ZIF-8/SALEM-2 hybrids calculated from the experimental transport diffusivities reported by Zhang and Koros[15] and the thermodynamic correction factors taken from simulated adsorption isotherms at 308 K.

ZIF	D_T [$cm^2\ s^{-1}$]	TCF [-]	D_0 [$cm^2\ s^{-1}$]
ZIF-8	2.3×10^{-18}	0.94	2.2×10^{-18}
ZIF-Im_{02}-mIm_{98}	5.7×10^{-18}	0.94	5.4×10^{-18}
ZIF-Im_{05}-mIm_{95}	1.7×10^{-17}	0.93	1.6×10^{-17}
ZIF-Im_{09}-mIm_{91}	2.9×10^{-17}	0.93	2.7×10^{-17}
ZIF-Im_{17}-mIm_{83}	9.2×10^{-16}	0.91	8.4×10^{-16}

Table S7. Corrected diffusivities of SF_6 in ZIF-8/SALEM-2 hybrids calculated from the experimental transport diffusivities reported by Zhang and Koros[15] and the thermodynamic correction factors taken from simulated adsorption isotherms at 308 K.

ZIF	D_T [$cm^2\ s^{-1}$]	TCF [-]	D_0 [$cm^2\ s^{-1}$]
ZIF-8	2.2×10^{-17}	1.11	2.4×10^{-17}
ZIF-Im_{02}-mIm_{98}	3.5×10^{-17}	1.11	3.9×10^{-17}
ZIF-Im_{05}-mIm_{95}	1.0×10^{-16}	1.10	1.1×10^{-16}
ZIF-Im_{09}-mIm_{91}	3.1×10^{-16}	1.09	3.4×10^{-16}
ZIF-Im_{17}-mIm_{83}	9.5×10^{-15}	1.08	1.0×10^{-14}

Supporting Information References

1. Clark, L. A.; Gupta, A.; Snurr, R. Q., Siting and Segregation Effects of Simple Molecules in Zeolites Mfi, Mor, and Bog. *J. Phys. Chem. B* **1998**, *102*, 6720-6731.
2. Zhang, L.; Hu, Z.; Jiang, J., Sorption-Induced Structural Transition of Zeolitic Imidazolate Framework-8: A Hybrid Molecular Simulation Study. *J. Am. Chem. Soc.* **2013**, *135*, 3722-3728.
3. Potoff, J. J.; Siepmann, J. I., Vapor–Liquid Equilibria of Mixtures Containing Alkanes, Carbon Dioxide, and Nitrogen. *AlChE J.* **2001**, *47*, 1676-1682.
4. Chen, B.; Potoff, J. J.; Siepmann, J. I., Monte Carlo Calculations for Alcohols and Their Mixtures with Alkanes. Transferable Potentials for Phase Equilibria. 5. United-Atom Description of Primary, Secondary, and Tertiary Alcohols. *J. Phys. Chem. B* **2001**, *105*, 3093-3104.
5. Martin, M. G.; Siepmann, J. I., Transferable Potentials for Phase Equilibria. 1. United-Atom Description of N-Alkanes. *J. Phys. Chem. B* **1998**, *102*, 2569-2577.
6. Wick, C. D.; Martin, M. G.; Siepmann, J. I., Transferable Potentials for Phase Equilibria. 4. United-Atom Description of Linear and Branched Alkenes and Alkylbenzenes. *J. Phys. Chem. B* **2000**, *104*, 8008-8016.
7. Dubbeldam, D.; Calero, S.; Vlugt, T. J. H.; Krishna, R.; Maesen, T. L. M.; Smit, B., United Atom Force Field for Alkanes in Nanoporous Materials. *J. Phys. Chem. B* **2004**, *108*, 12301-12313.
8. Jorgensen, W. L.; Laird, E. R.; Nguyen, T. B.; Tirado-Rives, J., Monte Carlo Simulations of Pure Liquid Substituted Benzenes with OPLS Potential Functions. *J. Comput. Chem.* **1993**, *14*, 206-215.
9. Castillo, J. M.; Vlugt, T. J. H.; Calero, S., Molecular Simulation Study on the Separation of Xylene Isomers in MIL-47 Metal−Organic Frameworks. *J. Phys. Chem. C* **2009**, *113*, 20869-20874.
10. Berendsen, H. J. C.; Grigera, J. R.; Straatsma, T. P., The Missing Term in Effective Pair Potentials. *J. Phys. Chem.* **1987**, *91*, 6269-6271.
11. Orsi, M., Comparative Assessment of the Elba Coarse-Grained Model for Water. *Mol. Phys.* **2014**, *112*, 1566-1576.
12. Zhang, C.; Lively, R. P.; Zhang, K.; Johnson, J. R.; Karvan, O.; Koros, W. J., Unexpected Molecular Sieving Properties of Zeolitic Imidazolate Framework-8. *J. Phys. Chem. Lett.* **2012**, *3*, 2130-2134.
13. Wu, H.; Gong, Q.; Olson, D. H.; Li, J., Commensurate Adsorption of Hydrocarbons and Alcohols in Microporous Metal Organic Frameworks. *Chem. Rev.* **2012**, *112*, 836-868.
14. Zhang, K.; Lively, R. P.; Zhang, C.; Chance, R. R.; Koros, W. J.; Sholl, D. S.; Nair, S., Exploring the Framework Hydrophobicity and Flexibility of ZIF-8: From Biofuel Recovery to Hydrocarbon Separations. *J. Phys. Chem. Lett.* **2013**, *4*, 3618-3622.
15. Zhang, C.; Koros, W. J., Tailoring the Transport Properties of Zeolitic Imidazolate Frameworks by Post-Synthetic Thermal Modification. *ACS Appl. Mater. Interfaces* **2015**, *7*, 23407-23411.
16. Dubbeldam, D.; Calero, S.; Ellis, D. E.; Snurr, R. Q., Raspa: Molecular Simulation Software for Adsorption and Diffusion in Flexible Nanoporous Materials. *Mol. Simul.* **2015**, 1-21.
17. Eum, K.; Jayachandrababu, K. C.; Rashidi, F.; Zhang, K.; Leisen, J.; Graham, S.; Lively, R. P.; Chance, R. R.; Sholl, D. S.; Jones, C. W.; et al. Highly Tunable Molecular Sieving and Adsorption Properties of Mixed-Linker Zeolitic Imidazolate Frameworks. *J. Am. Chem. Soc.* **2015**, *137*, 4191–4197.